SANDIA REPORT
SAND2018-10474
Unlimited Release
Printed September 2018

Current Loss in 0.1 - 100 Terawatt Vacuum Transmission Lines: Experiments and Simulations

Brian T. Hutsel, Jacy N. Gansz, Deanna M. Jaramillo, Diego J. Lucero, James K. Moore, David V. Rose, William A. Stygar

Prepared by
Sandia National Laboratories
Albuquerque, New Mexico 87185

Sandia National Laboratories is a multimission laboratory managed and operated by National Technology and Engineering Solutions of Sandia, LLC, a wholly owned subsidiary of Honeywell International, Inc., for the U.S. Department of Energy's National Nuclear Security Administration under contract DE-NA0003525.

Issued by Sandia National Laboratories, operated for the United States Department of Energy by National Technology and Engineering Solutions of Sandia, LLC.

Available to DOE and DOE contractors from

U.S. Department of Energy
Office of Scientific and Technical Information
P.O. Box 62
Oak Ridge, TN 37831

Telephone: (865) 576-8401
Facsimile: (865) 576-5728
E-Mail: reports@osti.gov
Online ordering: http://www.osti.gov/scitech

Available to the public from

U.S. Department of Commerce
National Technical Information Service
5301 Shawnee Rd
Alexandria, VA 22312

Telephone: (800) 553-6847
Facsimile: (703) 605-6900
E-Mail: orders@ntis.gov
Online order: https://classic.ntis.gov/help/order-methods/

SAND2018-10474
Printed September 2018
Unlimited Release

Current Loss in 0.1 - 100 Terawatt Vacuum Transmission Lines: Experiments and Simulations

Brian T. Hutsel, James K. Moore, William A. Stygar
Advanced Accelerator Physics

Diego J. Lucero, Deanna M. Jaramillo
Pulsed Power Engineering

Sandia National Laboratories
P. O. Box 5800
Albuquerque, New Mexico 87185

David V. Rose, Jacy N. Gansz

Voss Scientific
418 Washington St. SE
Albuquerque, New Mexico 87108

Abstract

Current loss in magnetically insulated transmission lines (MITLs) was investigated using data from experiments conducted on Z and Mykonos. Data from experiments conducted on Z were used to optimize an ion diode current loss model that has been implemented into the transmission line circuit model of Z. Details on the current loss model and comparisons to data from Z experiments have been previously published in a peer-reviewed journal [Hutsel, et al., Phys. Rev. Accel. Beams 21, 030401]. Dedicated power flow experiments conducted on Mykonos investigated current loss in a millimeter-scale anode-cathode gap MITL operated at lineal current densities greater than 410 kA/cm and with electric field stresses in excess of 240 kV/cm where it is expected that both anode and cathode plasmas are formed. The experiment MITLs were exposed to varying vacuum conditions; including vacuum pressure at shot time, time under vacuum, and vacuum storage protocols. The results indicate that the vacuum conditions have an effect on current loss in high lineal current density MITLs.

ACKNOWLEDGMENTS

The authors are extremely grateful to Eric Breden, Mike Cuneo, Dennis De Smet, David Justus, Aaron Lombrozo, Keven MacRunnels, Matt McCarthy, Jim Mignon, Jerry Mills, Tommy Mulville, Robert Speas, Michael Sullivan, and Adam York for their critical contributions and support of this effort. Supported by the Laboratory Directed Research and Development program at Sandia National Laboratories, a multi-mission laboratory managed and operated by National Technology and Engineering Solutions of Sandia, LLC, a wholly owned subsidiary of Honeywell International, Inc., for the U.S. Department of Energy's National Nuclear Security Administration under contract DE-NA0003525.

TABLE OF CONTENTS

1. Introduction 7
2. Mykonos experiment setup 8
   2.1. Pulsed power driver 8
   2.2. Load hardware design and processing 8
3. Experiment results 11
   3.1. Loss versus AK gap 11
   3.2. Loss versus vacuum conditions 13
4. Power flow simulations 16
   4.1. Bertha transmission line circuit model 16
   4.2. Chicago particle-in-cell simulations 19
5. Conclusions and future work 23
Appendix A: Experiment hardware revisons and results from initial hardware 24
   Hardware versions 24
   Initial experiment results 24
Appendix B: Shot log 28
References 31

FIGURES

Figure 1. Cross-section of Mykonos power flow experiment hardware. 9
Figure 2. Loss current versus AK gap for load hardware under vacuum for approximately 2 hours after installation. 11
Figure 3. Measured MITL currents and calculated loss currents for (a) 0.6 mm gap, (b) 0.8 mm gap, and (c) 1.0 mm gap MITLs. 12
Figure 4. Loss current versus vacuum pressure at shot time for a 1 mm AK gap MITL. 14
Figure 5. Loss current versus time under vacuum after installation for a 1 mm AK gap MITL. . 14
Figure 6. Measured MITL currents and calculated loss currents for (a) load hardware under vacuum for 5 minutes or less, (b) load hardware under vacuum for more than 2 hours, and (c) load hardware that was stored under vacuum prior to installation on Mykonos. 15
Figure 7. Overlay of simulated and measured data for shots there were under vacuum for (a) 18 hours and (b) 5 minutes. 17
Figure 8. Overlay of simulated and measured data for shots (a) 10067 with a 0.6 mm gap, (b) 10070 with a 0.8 mm gap, and (c) 10037 with a 1.0 mm gap. 18
Figure 9. Schematic of the equivalent circuit used to drive the Mykonos V PIC simulation. 19
Figure 10. Geometry setup for simulation (not to scale). 20

Figure 11. Upstream and downstream currents illustrating current loss in the MITL for (a) AK gap 0.6 mm, (b) AK gap 0.8 mm, and (c) AK gap 1.0 mm. 21

Figure 12. Electron density inside experimental AK gap at peak current (110ns) for the AK gap 0.6 mm. 22

Figure 13. Upstream and downstream current for a 0.6mm AK gap at (a) $1x10^{-5}$ Torr, (b) $2 x10^{-5}$ Torr. 22

Figure 14. Two sets of experiment hardware sets tested. (a) initial experiments used a cathode rod with a slip contact into the cathode cone upstream of the rod. (b) final experiments used a single piece cathode to remove the current contact upstream of the experiment MITL. 25

Figure 15. Loss current versus vacuum pressure at shot time for a 1 mm AK gap MITL using the initial hardware configuration. 26

Figure 16. Loss current versus time under vacuum after installation on Mykonos for a 1 mm AK gap MITL using the initial hardware version. 27

TABLES

Table 1. Mykonos shot log for MITL power flow experiments. 28

1. INTRODUCTION

Magnetically insulated transmission lines (MITLs) are often used in the final stages of pulsed power systems to transfer energy at high voltage and current to an experiment load [1]. Understanding power flow in these high-energy density regions is critical for determining the power coupling between the pulsed power accelerator and the load. In pulsed power accelerators like the Z machine [2,3], the final stages of the MITLs prior to the load are operated at lineal current densities exceeding 400 kA/cm. At this threshold Ohmic heating alone is expected to increase conductor temperatures enough to desorb contaminates from electrodes leading to electrode plasma formation [4,5]. In addition to Ohmic heating, charged particle impacts may further increase electrode temperatures. In this Laboratory-Directed Research and Development (LDRD) project, power flow in MITLs operated at current densities exceeding 400 kA/cm were studied. Data from experiments conducted on Z and Mykonos [6-8] were used.

Data from experiments conducted on Z were used to optimize a current loss model that has been implemented into the transmission line circuit model of Z. Details on the current loss model and comparisons to Z data have been published in a peer-reviewed journal and will not be repeated in this report [9].

Dedicated power flow experiments were conducted on the Mykonos LTD accelerator. Mykonos was used to drive MITL electrodes with lineal current densities in excess of 400 kA/cm leading to anode plasma formation. The experiments focused on determining the effect of vacuum conditions on the current loss observed. The high lineal current density experiments presented here are a follow-on to prior experiments on Mykonos that investigated power flow at low (<50 kA/cm) lineal current densities [10]. The low current density experiments did not show any dependence on vacuum conditions, possibly because there was not sufficient electrode heating to remove contaminates from electrode surfaces. The high lineal current density experiments were designed to test if vacuum conditions at shot time would affect contaminate inventories and lead to a delay, or elimination of, anode plasma formation and current loss in the MITL. In addition to the experiments, circuit model simulations using Bertha [11] and particle-in-cell simulations using Chicago [12] of the Mykonos experiments were conducted to compare models of current loss to the experiment data.

The remainder of this report is divided into 4 additional sections. Section 2 describes the MITL power flow experiments conducted on Mykonos. Section 3 presents the experiment results. Section 4 presents the circuit model and particle-in-cell simulations of the Mykonos experiments. Section 5 concludes the report and describes potential future work. Two Appendices are included as well. Appendix A describes two versions of the experiment hardware and shows the inconsistent results from the initial hardware version that lead to a hardware revision. Appendix B contains a shot log for the Mykonos experiments.

2. MYKONOS EXPERIMENT SETUP

2.1. Pulsed power driver

The Mykonos linear transformer driver (LTD) module served as the pulsed power driver for the MITL power flow experiments. The Mykonos LTD module is made up of five, three-meter diameter, LTD cavities. Each cavity contains of 36 LTD bricks, each built with a HCEI 200 kV multi-gap switch [13] and two 40 nF General Atomics 31165 capacitors. The five cavities are triggered sequentially and drive a matched impedance coaxial water transmission line. The cavities are triggered with a 6.6 ns delay between cavities to match the transit time of the power pulse in the water transmission line. The LTD cavities are designed to operate at up to ±100 kV charge voltage. At full charge voltage, Mykonos nominally produces a 1 MA, 500 kV pulse with a rise time (10-90) of 60 ns and a pulse width (FWHM) of 160 ns into a 0.5 Ω matched load. The noted references contain additional details on the Mykonos LTD cavities [14] and the two-cavity module [6-8] that preceded the five-cavity module.

2.2. Load hardware design and processing

The Mykonos experiments were designed to test power flow in a MITL at lineal current densities sufficient to heat the conductor surfaces above the threshold for anode plasma formation and ion emission. References [4,5] suggest that a temperature rise of 400±60 °C is sufficient to form an anode plasma. According to [15], the electrode temperature rise can be estimated by

$$\Delta T = \frac{\vartheta B^2(t)}{2\mu_0 c_v}, \tag{1}$$

where ϑ is a dimensionless surface energy factor, B is the magnetic field, μ_0 is the permittivity of free space and c_v is the specific heat per unit volume of the electrode material. In our analysis, assuming stainless steel conductors and a linear current rise,

$$c_v = 3.37 \times 10^6 \ \mathrm{J/(m^3 \cdot K)}, \tag{2}$$

$$\vartheta = 1.273. \tag{3}$$

With the magnetic field given by

$$B = \frac{\mu_0 I}{2\pi r}, \tag{4}$$

equations (1)-(4) can be combined to solve for a lineal current density of 410 kA/cm necessary to raise the electrode temperature 400 °C. This lineal current density limit was used to set a maximum size of the MITL electrodes that would be expected to form anode plasmas.

A cross-section view of the vacuum hardware is shown in Figure 1. A radial water transmission line, vacuum insulator, and radial vacuum transmission line served to direct power flow to the small diameter of the MITL being tested. The vacuum insulator serves to isolate the water-insulated transmission line from the vacuum-insulated transmission line. The vacuum insulator was also designed to direct power flow through

a series water resistor. This water resistor was adjustable from 0.1 Ω to 0.5 Ω and was used to dampen reflections back into the cavities from the short-circuit inductive load.

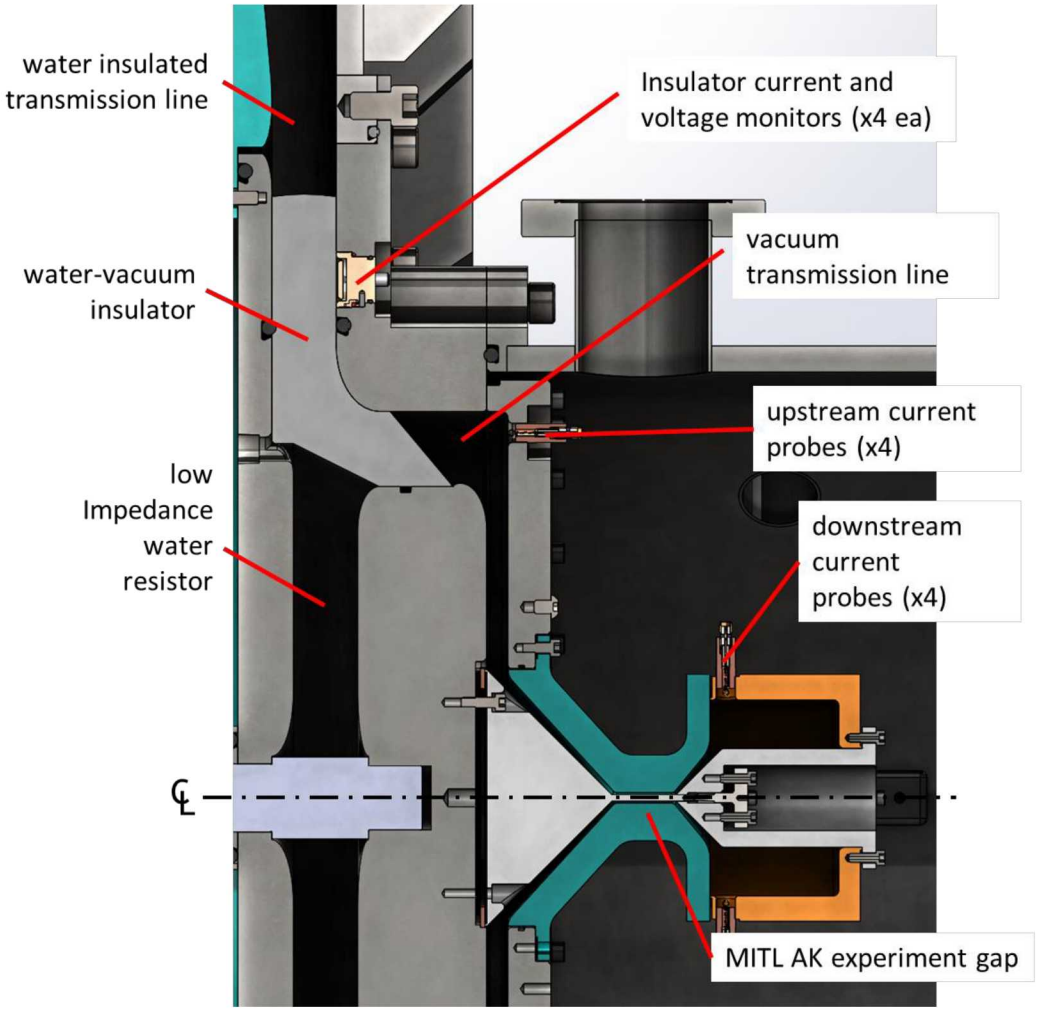

Figure 1. Cross-section of Mykonos power flow experiment hardware.

The experiment MITL consisted of a 3 cm long coaxial vacuum transmission line. Initial shots varied both the anode radius, cathode radius, and the load inductance to find an appropriate operating point. After the initial experiments, the cathode radius was fixed at 1.5 mm. The anode radius was varied between 2.1 mm and 2.5 mm, resulting in anode-cathode (AK) gaps of 0.6, 0.8, or 1.0 mm. A constant 10 nH inductance served as the load downstream of the experiment gap. The gap was designed to operate at electric fields well above of 240 kV/cm where explosive electron emission from the cathode is expected [16]. The anode radius was chosen to permit lineal current densities in excess of 410 kA/cm necessary for Ohmic heating to increase the electrode temperatures more than 400 °C and form anode plasmas. Mykonos produced a peak current of approximately 850 kA into the designed load. Using the anode sizes listed above, it is expected that the 400 °C temperature threshold would be reached between

540 kA and 700 kA. If there is additional heating to the anode surface from charged particle impacts, the temperature threshold could be reached earlier in the current pulse.

The primary power flow diagnostics included B-dot and D-dot monitors to measure current and voltage. Four B-dots and four D-dots were located at the vacuum insulator. These monitors were identical to those described in Sections III and V of [17]. In the vacuum transmission line, a total of eight B-dots were used to measure current. Four were located upstream and four were located downstream of the experiment MITL. The vacuum B-dots were designed as a 2-loop version of the inner-MITL current monitor described in Section IV of [17]. Vacuum pressure was measured using an MKS 979b vacuum gauge.

The experiment gap anode and cathode were made of stainless steel 304L. The anode and cathode were machined with no cutting oil and electropolished per ASTM B912 standards. After machining, the hardware was cleaned with isopropanol and a TX309 Texwipe, rinsed with isopropanol, blown dry with nitrogen, vacuum baked at 800 °C for four hours, and finally wrapped in a TX309 Texwipe and All-Foils UHV aluminum foil.

3. EXPERIMENT RESULTS

The experiments conducted on Mykonos looked at current loss as a function of AK gap size and the vacuum history of the load hardware.

3.1. Loss versus AK gap

The MITL AK gap was varied between 0.6 and 1.0 mm. Consistent with previous work at low lineal current densities [10], the MITL AK gap had a large influence on current loss. Figure 2 shows data from experiments with 0.6, 0.8, and 1.0 mm AK gaps. The vacuum conditions for all the shots in Figure 2 were nominally the same with a 2 hour pump down prior to shooting. The measured currents before and after the MITL, and the calculated loss currents for these shots are shown in Figure 3. It can be seen that the loss current begins at roughly 200 ns for all three gap sizes. Larger gaps are able to pass current longer prior to completely shorting out. Shorting across the MITL AK gap is indicated by the downstream B-dot signal flat-lining, then slowly L/R over several microseconds (not shown in Figure 3). The 1.0 mm gap had very little current loss and MITL AK gap shorting was delayed until after peak current when the voltage on the MITL reverses.

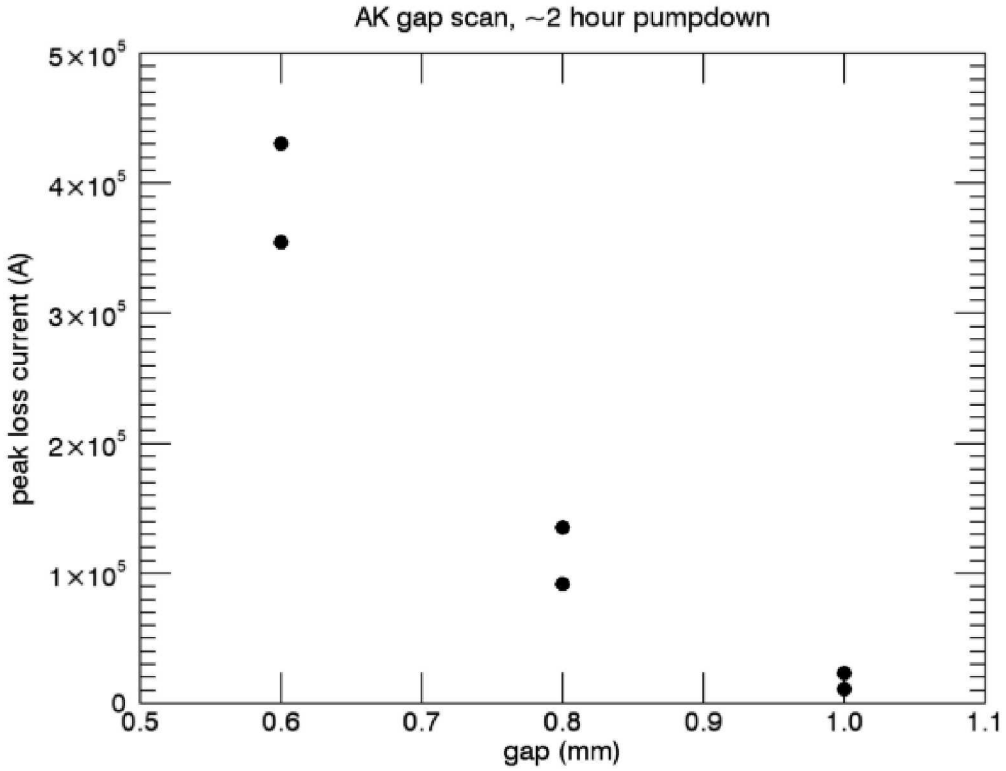

Figure 2. Loss current versus AK gap for load hardware under vacuum for approximately 2 hours after installation.

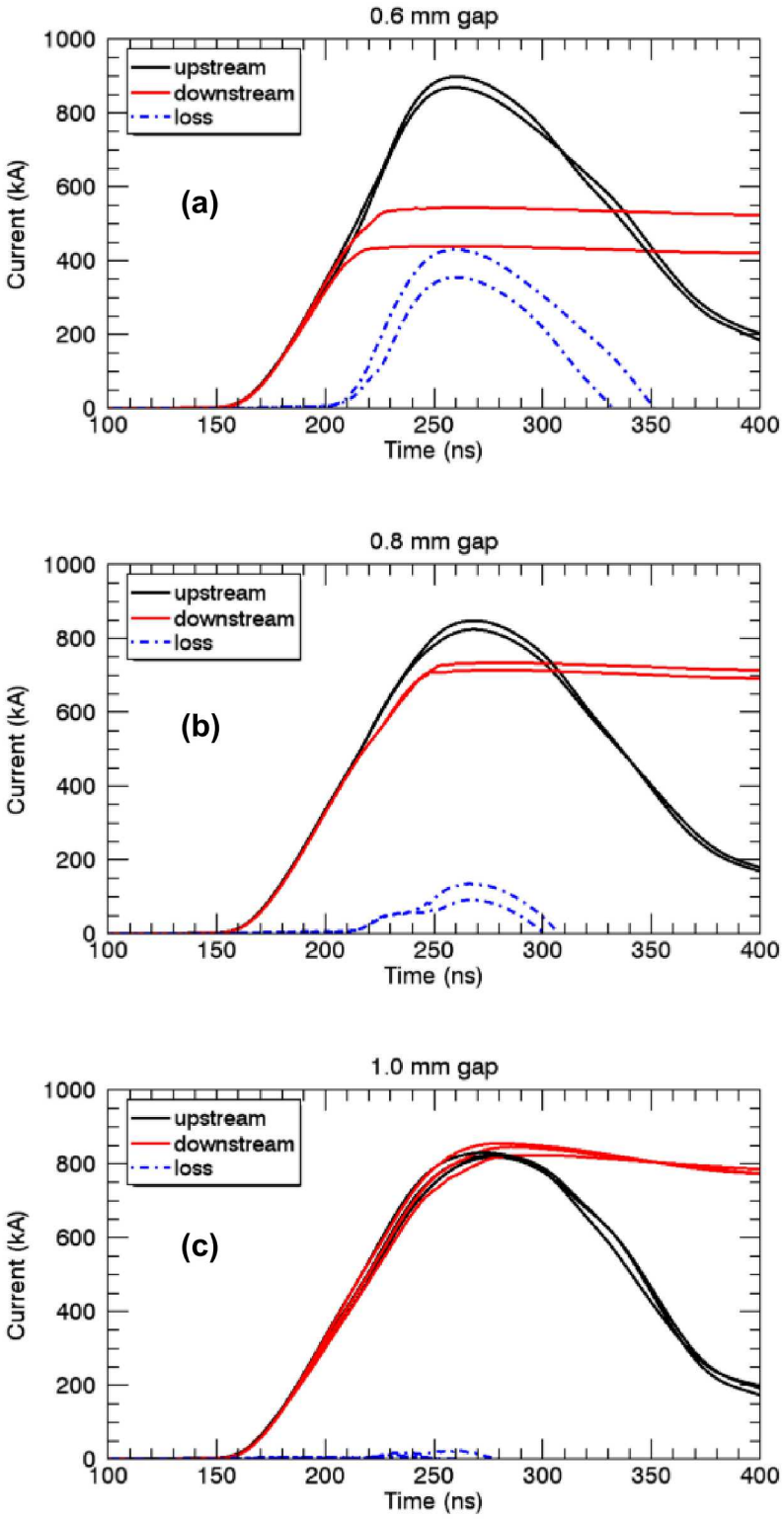

Figure 3. Measured MITL currents and calculated loss currents for (a) 0.6 mm gap, (b) 0.8 mm gap, and (c) 1.0 mm gap MITLs.

3.2. Loss versus vacuum conditions

The vacuum conditions of the MITL (time under vacuum and/or vacuum pressure) after load hardware installation and the effect of storing load hardware in a separate vacuum chamber prior to installation were tested using the 1.0 mm AK gap.

Figures 4 and 5 show the peak current loss measured on these shots. Figure 4 shows the current loss as a function of vacuum pressure at shot time. Figure 5 shows the current loss as a function of time under vacuum after load hardware installation and prior to the shot. The measured currents before and after the MITL, and the calculated loss currents for these shots are shown in Figure 6. The blue data markers in Figures 4 and 5 show shots taken with load hardware that was stored in the Mykonos high bay (wrapped in aluminum foil after cleaning and vacuum baking). The time under vacuum after installation and prior to the shot was varied from 5 minutes to 5 days. The highest loss was seen for shots taken at higher base pressures or shorter time under vacuum after installation. Load hardware that was under vacuum for 2 hours or more after installation had very little current loss and MITL AK gap shorting was delayed until after peak current when the voltage on the MITL reverses. Data shown with red markers in Figures 4 and 5 represent shot hardware that was stored in a separate vacuum chamber prior to installation on the machine. Hardware was removed from the storage chamber immediately before installing on the machine. The four shots with the lowest loss were exposed to the high bay atmosphere for approximately 30 minutes during installation. The single vacuum storage point near 100 kA peak loss was exposed to the high bay atmosphere for approximately 2 hours during installation. Load hardware stored under vacuum prior to installation on Mykonos was only left under vacuum for less than 10 minutes after installation on Mykonos prior to the shot. Vacuum pressure at shot time ranged from 5×10^{-4} Torr to 5×10^{-5} Torr for the shots with load hardware that was stored under vacuum prior to installation on Mykonos.

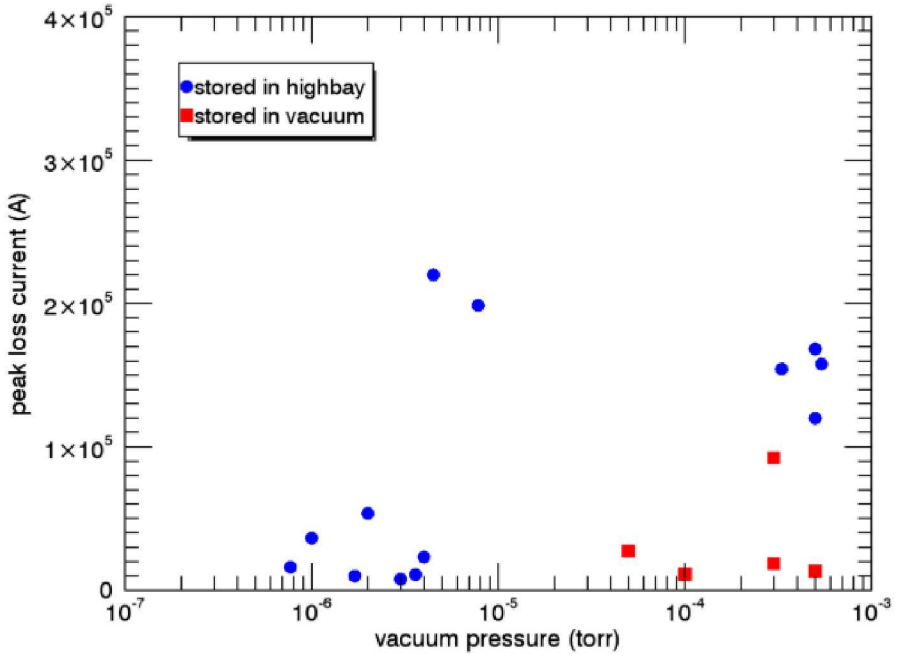

Figure 4. Loss current versus vacuum pressure at shot time for a 1 mm AK gap MITL.

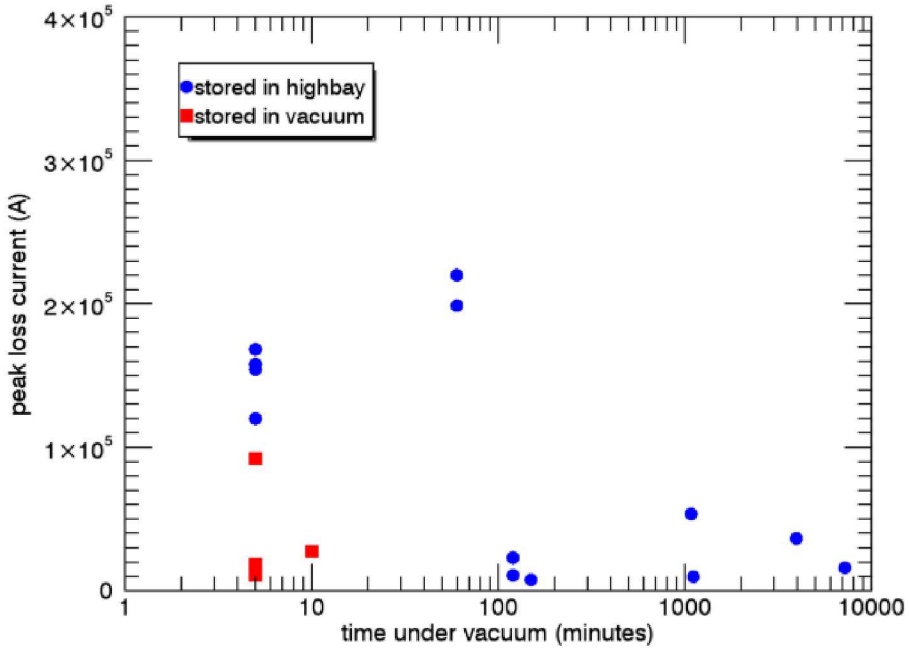

Figure 5. Loss current versus time under vacuum after installation for a 1 mm AK gap MITL.

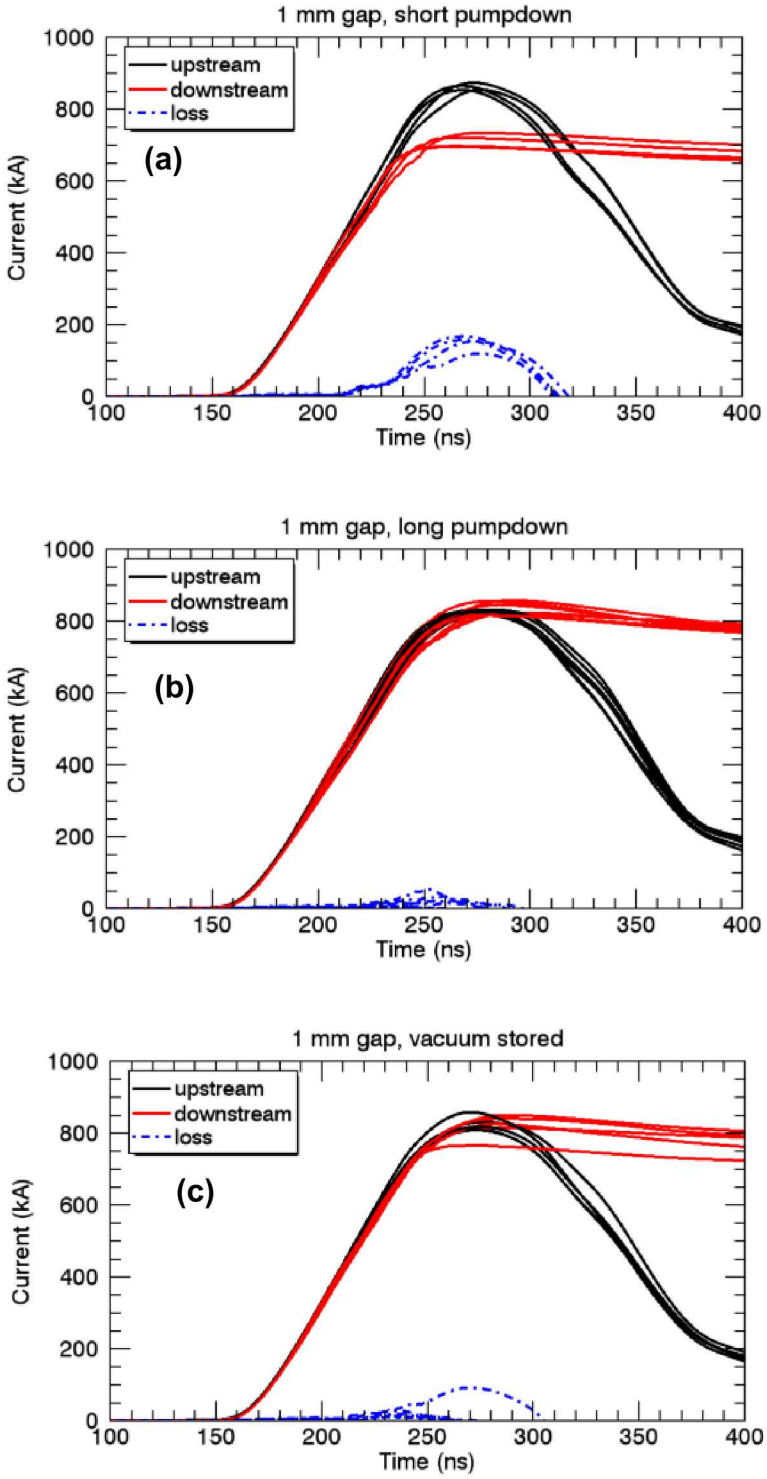

Figure 6. Measured MITL currents and calculated loss currents for (a) load hardware under vacuum for 5 minutes or less, (b) load hardware under vacuum for more than 2 hours, and (c) load hardware that was stored under vacuum prior to installation on Mykonos.

4. POWER FLOW SIMULATIONS

4.1. Bertha transmission line circuit model

Transmission line circuit simulations of several Mykonos experiments were done using Bertha [11]. The simulations used the same MITL current loss model that is implemented in the Z circuit model [9]. One difference in the Mykonos simulations is that the turn on time of anode emission was varied from 400 °C with the assumption that anode plasma turn on time is varying with the vacuum conditions. Additionally, in the Mykonos simulations, ion emission from the anode is assumed to have no enhancement due to negative space charge (i.e. the enhancement factor is 1).

Figure 7 shows simulations of two 1.0 mm AK gap shots with different time under vacuum prior to the shot. Shot 10037 in Figure 7a was under vacuum overnight (18 hours) prior to shooting. Shot 10040 in Figure 7b was under vacuum for only 5 minutes prior to shooting. In the simulations, earlier gap closure with higher pressure is accounted for by reducing the turn on temperature threshold for anode plasma formation.

Figure 8 shows simulations of shots with AK gaps of 0.6, 0.8, and 1.0 mm. In this case, the vacuum conditions during all three shots were similar. The load was not stored under vacuum prior to installation on Mykonos and after installation the load hardware was under vacuum for approximately 2 hours prior to the shot. Simulations of the shots in Figure 8 use the same turn on temperature for the anode ion emission. However, since the AK gap size was adjusted by changing the anode radius, it is expected that shots with the smaller AK gaps will reach the threshold temperature earlier in the current pulse.

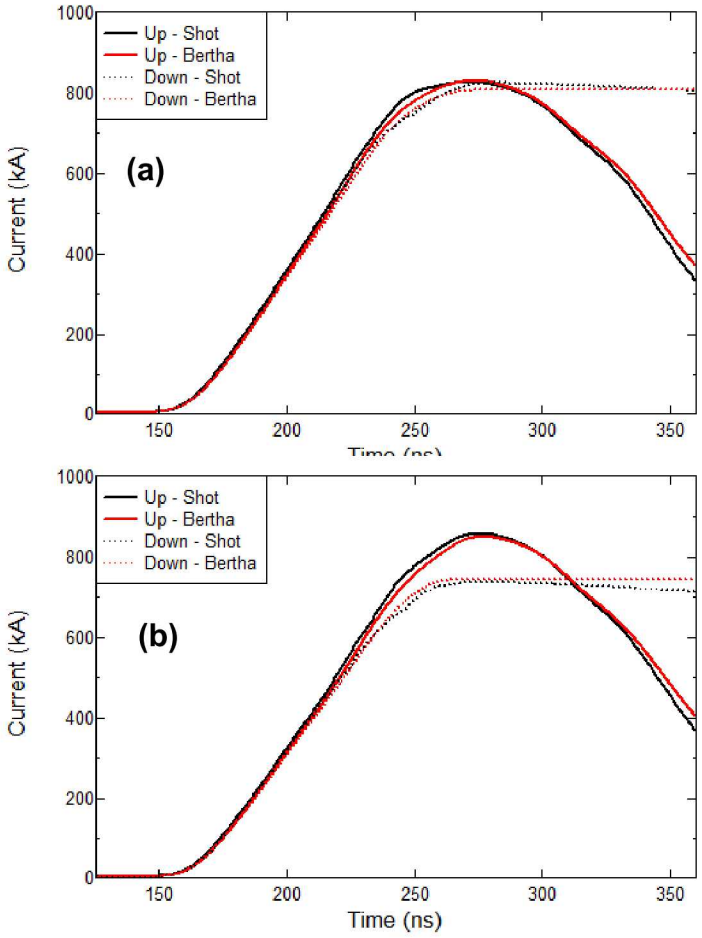

Figure 7. Overlay of simulated and measured data for shots there were under vacuum for (a) 18 hours and (b) 5 minutes.

.

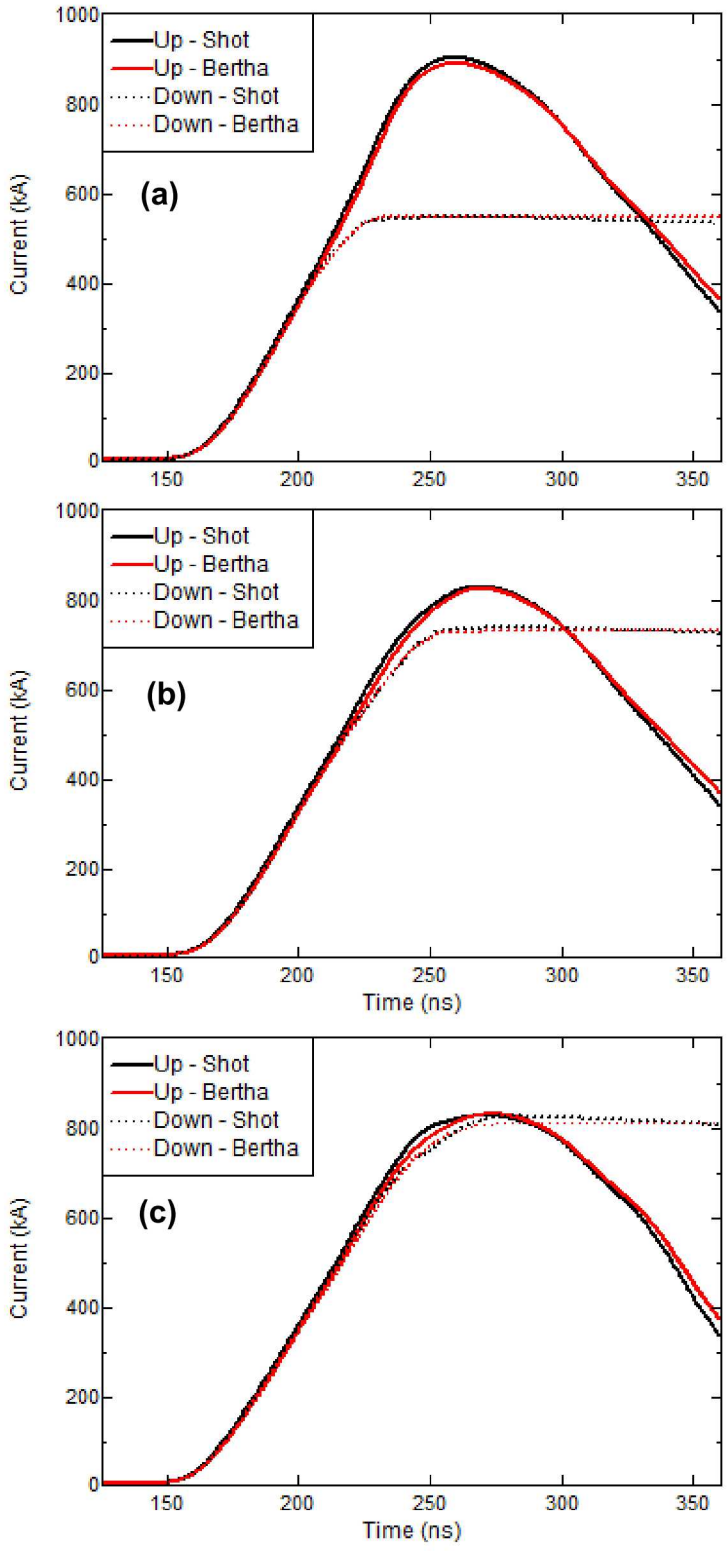

Figure 8. Overlay of simulated and measured data for shots (a) 10067 with a 0.6 mm gap, (b) 10070 with a 0.8 mm gap, and (c) 10037 with a 1.0 mm gap.

4.2. Chicago particle-in-cell simulations

Utilizing the particle-in-cell (PIC) code Chicago [12], a 2D (r,z) cylindrical, fully kinetic, fully electromagnetic simulation model was used to model the Mykonos experiment MITL. Power is driven from the upstream side by a circuit that represents the 5 LTD cavities, the water transmission line, and the water resistor that are upstream of the vacuum section on Mykonos V. The circuit schematic is shown in Figure 9. Geometry of the simulation is seen in Figure 10. The cell size in the AK gap is 200 microns (Δz) by 70 microns (Δr) inside the MITL region. The time step is dynamically adjusted to satisfy numerical constraints.

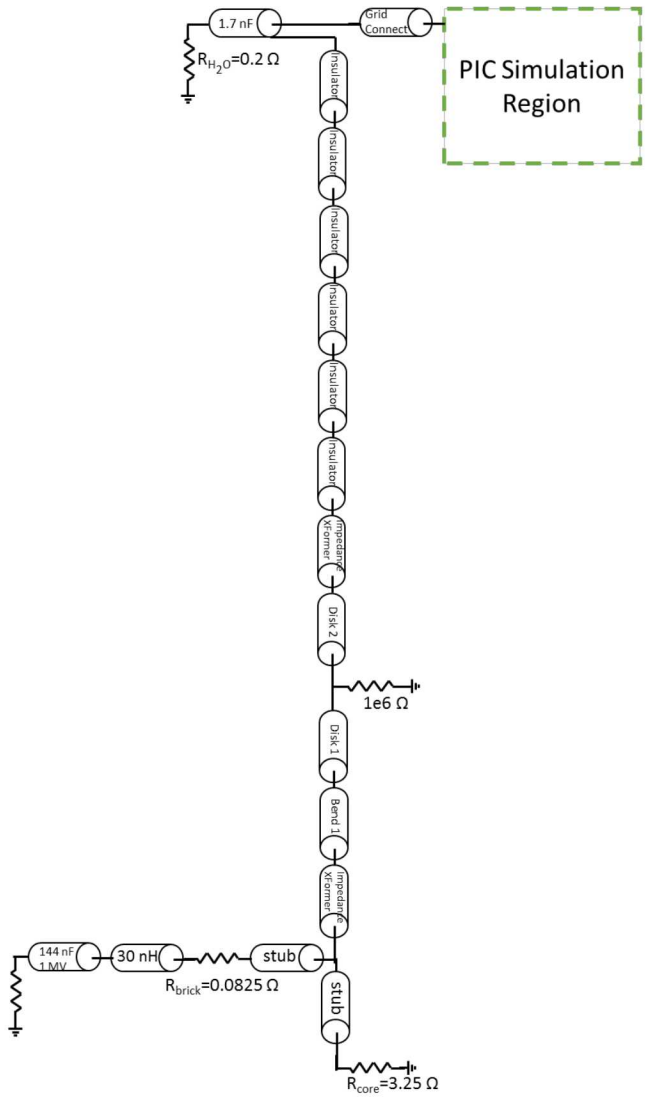

Figure 9. Schematic of the equivalent circuit used to drive the Mykonos V PIC simulation.

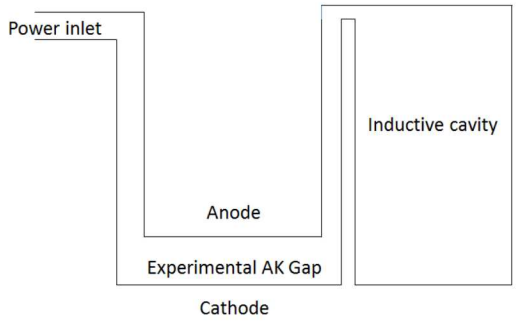

Figure 10. Geometry setup for simulation (not to scale).

The cathode radius is fixed at 1.5 mm. Cathode electron emission is enabled in the coaxial MITL when electric field stress along the electrode surface exceeds a set value of 240 kV/cm [16]. Cathode plasma formation in the simulation is triggered by the same electric field stress value. Anode plasma creation is allowed for anode surfaces that exceed a temperature increase of 400 °C or more. The plasma creation model is newly formulated for Z convolute simulations and will be described elsewhere [18]. The plasma creation models for both cathodes and anodes are based on the Temkin isotherm [19] with a vacuum pressure of 10^{-5} Torr unless stated otherwise. The neutral desorption rate is then self-consistently calculated based on that pressure. The explosive emission of neutrals from the conductor surfaces is followed by a fragmentation process where the neutrals are broken into positive and negative components. For these simulations the neutrals desorbed are water (H_2O) that are fragmented into O^+, H^+, and e^-.

Current loss was examined for the three different AK gap settings, 0.6 mm, 0.8 mm and 1.0 mm. The downstream current and upstream current are plotted for all 3 cases in Figure 11. As expected the largest loss was seen in the 0.6 mm AK gap and smallest loss in the 1.0 mm AK gap. Peak current was achieved at approximately 110 ns. After 140 ns, electrons begin to stream across from cathode to anode as the voltage falls to zero and then changes sign. Magnetic insulation is set up very rapidly in these simulations due to the high magnetic fields at the 1.5 mm radius cathode.

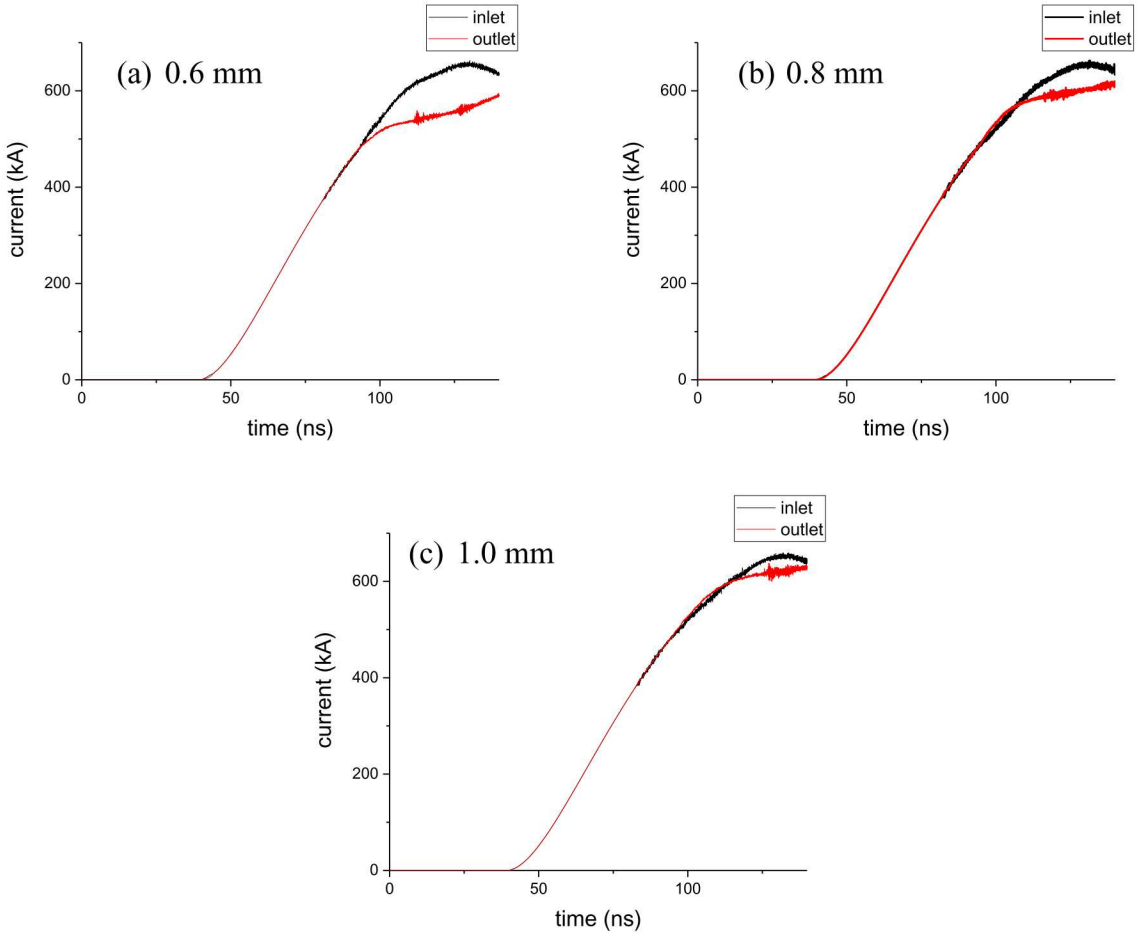

Figure 11. Upstream and downstream currents illustrating current loss in the MITL for (a) AK gap 0.6 mm, (b) AK gap 0.8 mm, and (c) AK gap 1.0 mm.

At early times (up to ~80 ns) there is no difference between upstream (inlet) and downstream (outlet) currents, illustrating that there is no current loss due to electrons or ions crossing the AK gap. Nearing the time of peak current, electrons cross the AK gap resulting in current loss. This loss is driven by electrode plasma expansion in the AK gap. Figure 12 shows the electron number density at t=110 ns for the 0.6 cm AK gap case. The electron sheath fills the AK gap, resulting is significant current loss at this time.

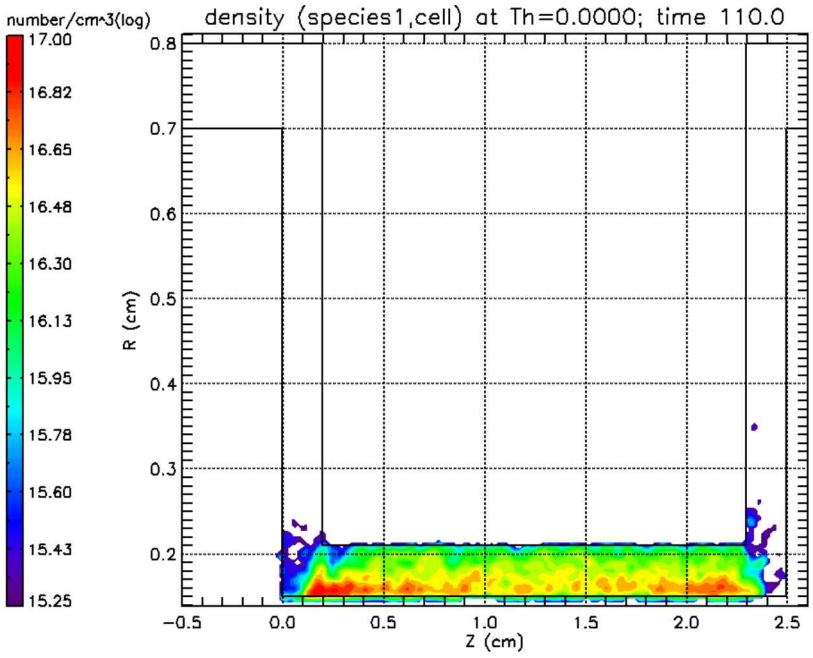

Figure 12. Electron density inside experimental AK gap at peak current (110ns) for the AK gap 0.6 mm.

Additional simulations were carried out to investigate the current loss dependence on vacuum pressure. Simulations with higher vacuum pressure were run for AK gap sizes of 0.6 mm, 0.8 mm, and 1 mm. The vacuum pressure was increased from $1x10^{-5}$ Torr to $2x10^{-5}$ Torr. For all cases, this increase in the vacuum pressure does not have a significant impact of the initiation time of current loss or the overall magnitude. This is illustrated in Figure 13 for the 0.6 mm AK gap.

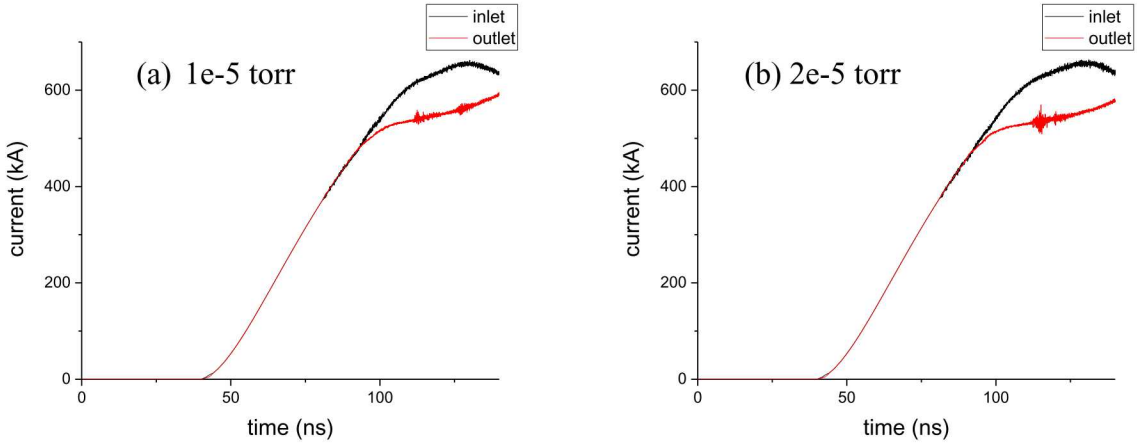

Figure 13. Upstream and downstream current for a 0.6mm AK gap at (a) $1x10^{-5}$ Torr, (b) 2 $x10^{-5}$ Torr.

5. CONCLUSIONS AND FUTURE WORK

Current loss in high current density MITLs was evaluated using data from experiments conducted on Z and Mykonos. Data from Z experiments were used to optimize a model of current loss in at MITL that was implemented into the transmission line circuit model of Z. As shown in [9], simulations using the current loss model agree with measurements on Z to within 2% for a variety of Z experiments. Dedicated power flow experiments on a high current density cylindrical MITL were conducted on the Mykonos LTD. The experiment MITLs were designed to reach threshold temperatures required to form electrode plasmas. Current loss was evaluated for MITL AK gaps of 0.6 mm – 1.0 mm. Current loss was also evaluated for various vacuum conditions at shot time with a 1.0 mm AK gap. Shots were taken with base pressures ranging between $7x10^{-4}$ Torr - $7x10^{-7}$ Torr with vacuum pump down times between 5 minutes and 5 days. The experiments reveal that increased time under vacuum and/or lower base pressures improves current delivery through the MITL. Experiments also revealed that the benefits of long pump down times can be realized by storing the MITL under vacuum prior to installing the hardware for the experiment. Load hardware that was stored in an offline vacuum chamber at pressures near 10^{-7} Torr for at least 2 days and exposed to atmosphere for only a short time (approximately 30 minutes) during installation had similar (negligible) current loss to hardware that was installed on the machine for more than 2 hours. The current loss was similar despite vacuum stored hardware shots taken at base pressures 2 orders of magnitude higher than the long pumpdown hardware, $5x10^{-4}$ Torr compared to $5x10^{-6}$ Torr.

Further work could be done to characterize the electrode surfaces after being exposed to the various vacuum protocols to attempt to connect MITL power flow to electrode surface conditions. It would be of interest to test alternative electrode materials. On Z, some load hardware is made from aluminum. The experiments could be repeated with aluminum anodes to determine if the current loss is significantly different with aluminum instead of stainless steel. It would also be interesting to see if the large power flow differences observed still apply at higher current densities. It may be that the differences seen are only apparent due to the relatively slow rate of temperature rise. It is expected that the anode plasma turn on time would vary 10's of ns for small differences in temperature changes. On a larger, higher current, accelerator like Z, the anode temperature rate of rise is much faster since Ohmic heating is proportional to I^2, and the difference in anode turn on time may only be a few ns. Additional simulation work in both Bertha and Chicago will be needed to adjust the anode plasma formation models based on the experimental data. Bertha currently assumes an anode plasma turn on temperature threshold and Chicago assumes that contaminate desorption is a function of vacuum pressure at shot time. Neither model would account for the differences in anode plasma formation time that was seen when load hardware stored under vacuum prior to installation. Instead the anode plasma formation needs to be a function of electrode surface conditions.

APPENDIX A: EXPERIMENT HARDWARE REVISONS AND RESULTS FROM INITIAL HARDWARE

Hardware versions

The two versions of experiment hardware are show in Figure 14. Figure 14a shows the initial experiment hardware used in shots with shot numbers less than 9980. Figure 14b shows the revised experiment hardware used in shots with shot numbers greater than 10036.

Initial experiment results

The initial experiments used the hardware depicted in Figure 14a. These experiments varied both the MITL anode and cathode radius to determine the appropriate AK sizes and gaps for further study. It was determined that gaps of 1 mm or less were necessary to see any current loss, regardless of vacuum conditions.

The experiment results using the initial hardware sets produced inconsistent current loss from shot to shot. The inconsistent results were assumed to be caused by the slip fit current contact between the conical transition to small radius and the cathode rod of the experiment MITL. As specified, the maximum distance between the cathode rod and cone was less than 0.0025". Discharges and plasma formation at this contact may vary greatly from shot to shot leading to erratic differences in power flow through the MITL. This can be seen in Figures 15 and 16 which show the peak current loss as a function of vacuum pressure and time under vacuum. It can be seen that, independent of vacuum conditions, the current loss in the MITL could vary from negligible loss to losses of over 250 kA. It is also noted that the experiment results using the initial hardware version were conducted at a lower charge voltage which produced a peak current of only approximately 600 kA. This peak current was near the threshold for anode plasma formation. If these initial experiments were consistent with the experiments that used the revised hardware presented in Section 3, we would expect to see negligible losses until just near peak current for all vacuum conditions.

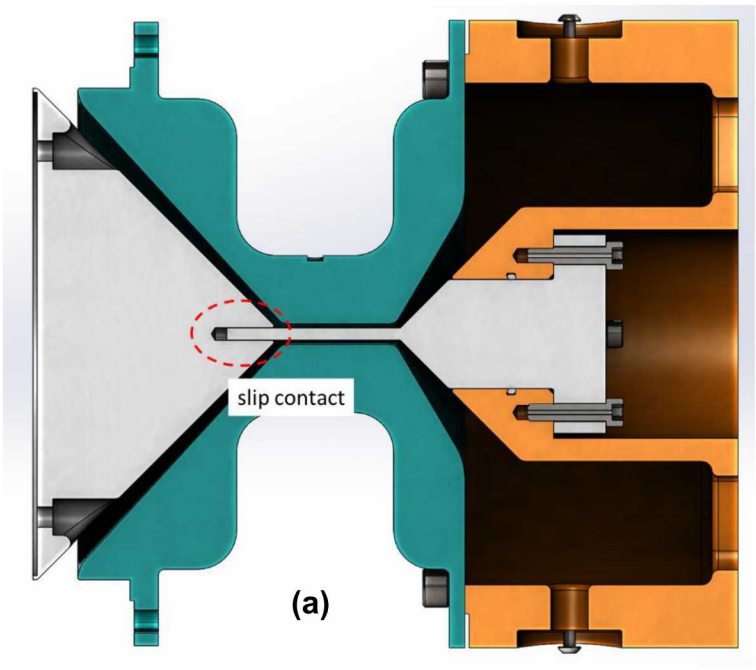

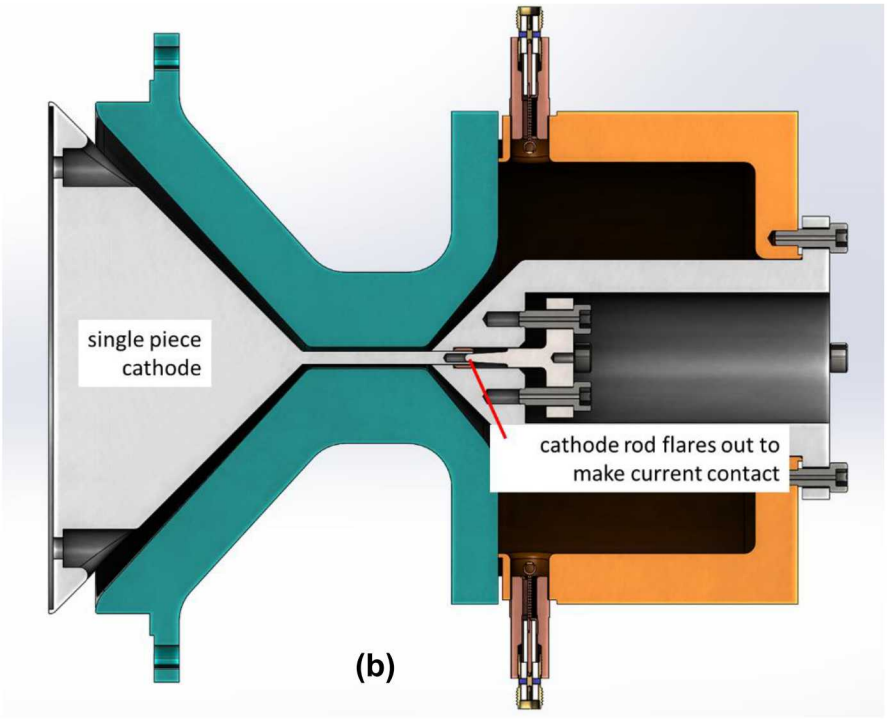

Figure 14. Two sets of experiment hardware sets tested. (a) initial experiments used a cathode rod with a slip contact into the cathode cone upstream of the rod. (b) final experiments used a single piece cathode to remove the current contact upstream of the experiment MITL.

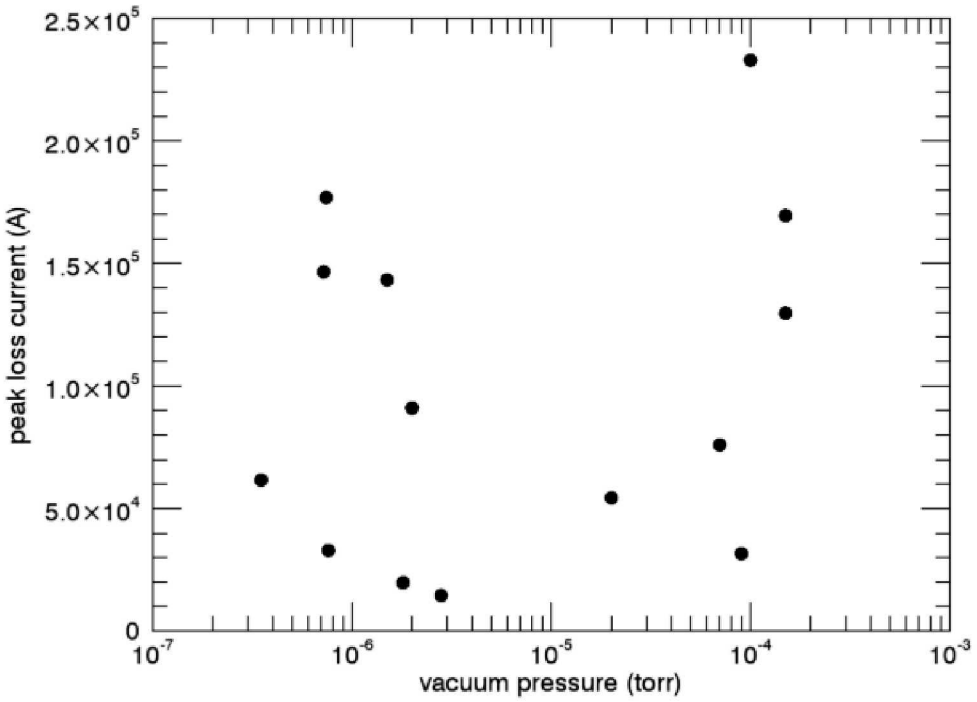

Figure 15. Loss current versus vacuum pressure at shot time for a 1 mm AK gap MITL using the initial hardware configuration.

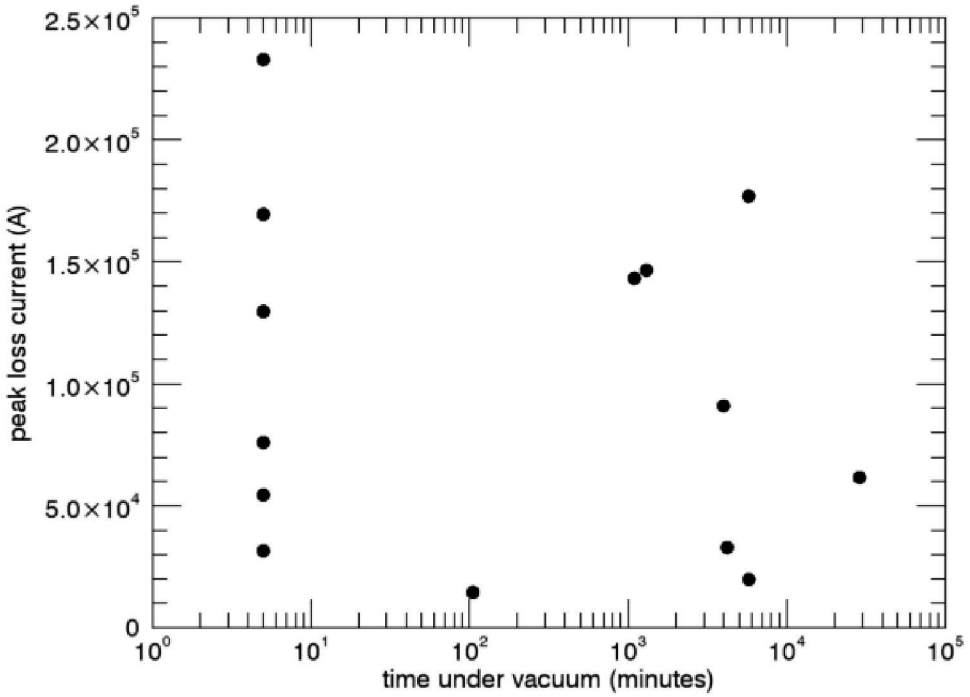

Figure 16. Loss current versus time under vacuum after installation on Mykonos for a 1 mm AK gap MITL using the initial hardware version.

APPENDIX B: SHOT LOG

The following table is a record of the shots taken on Mykonos with the high current density MITL hardware. Shots 9980 and earlier used the initial version of the experiment hardware. Shots 10036 used the revised version of the experiment hardware. "Time under vacuum" refers to the time between turning on the turbo pump after installing the load hardware on Mykonos and the shot time. "Time between vacuum storage and install" is only applicable to shots where the load hardware was stored in a separate vacuum chamber and lists the approximate time between removing the hardware from storage and completing the hardware installation on Mykonos.

Table 1. Mykonos shot log for MITL power flow experiments.

Shot	Gap [mm]	Cathode radius [mm]	Vcharge [kV]	Vac [Torr]	Time under vacuum [min]	Time between vacuum storage and install [min]	Load conductivity [mS/cm]
9844	4.0	1.5	60	2.5E-6	1440	-	35.0
9845	2.0	1.5	60	2.5E-6	1440	-	32.0
9846	1.0	1.5	60	1.8E-6	5775	-	32.0
9847	1.0	1.5	60	7.0E-5	5	-	32.0
9848	1.0	1.5	60	9.0E-5	5	-	32.0
9849	2.0	1.5	60	6.0E-5	5	-	32.0
9850	3.0	1.5	60	8.0E-5	5	-	32.0
9851	1.0	1.5	60	2.0E-6	3990	-	32.0
9852	2.0	1.5	60	2.0E-6	3990	-	32.0
9853	2.0	1.5	60	3.0E-6	1440	-	32.0
9954	4.0	1.5	60	2.0E-6	2500	-	31.1
9955	1.0	1.5	60	2.8E-6	105	-	17.6
9956	1.0	1.5	60	3.5E-7	28800	-	17.3
9957	1.0	1.5	60	2.0E-5	5	-	18.0
9958	1.0	2.5	60	4.3E-7	4320	-	18.0
9960	1.0	2.0	60	4.8E-7	5760	-	18.2
9961	1.0	2.0	60	2.0E-5	5	-	18.2
9962	0.75	1.5	70	5.0E-7	1020	-	17.8
9963	1.0	2.0	60	5.0E-7	1020	-	18.3
9964	0.75	1.5	60	5.0E-5	5	-	19.0
9965	0.75	1.5	60	4.5E-7	5462	-	19.2
9966	1.0	2.0	80	7.0E-5	5	-	19.1

Shot	Gap [mm]	Cathode radius [mm]	Vcharge [kV]	Vac [Torr]	Time under vacuum [min]	Time between vacuum storage and install [min]	Load conductivity [mS/cm]
9967	1.0	2.0	80	5.2E-7	5887	-	19.4
9968	1.0	2.5	80	8.6E-5	5	-	19.3
9969	1.0	2.5	80	9.0E-7	1432	-	19.6
9970	0.75	1.5	80	6.6E-7	1324	-	19.8
9971	0.75	1.5	80	4.0E-4	5	-	19.8
9972	1.0	2.0	90	5.0E-7	5404	-	20.3
9973	1.0	2.5	90	5.0E-7	3000	-	20.4
9974	1.0	1.5	90	1.5E-6	1092	-	20.3
9975	1.0	1.5	90	7.6E-7	4212	-	20.4
9976	1.0	1.5	90	7.2E-7	1302	-	20.6
9977	1.0	1.5	90	1.0E-4	5	-	20.5
9978	1.0	1.5	80	1.5E-4	5	-	20.6
9979	1.0	1.5	80	7.4E-7	5760	-	20.6
9980	1.0	1.5	80	1.5E-4	5	-	20.0
10036	1.0	1.5	80	4.0E-6	120	-	19.9
10037	1.0	1.5	80	2.0E-6	1080	-	19.9
10038	1.0	1.5	80	7.8E-6	60	-	20.0
10039	1.0	1.5	80	1.7E-6	1110	-	20.0
10040	1.0	1.5	80	5.0E-4	5	-	20.0
10046	1.0	1.5	80	3.3E-4	5	-	20.0
10047	1.0	1.5	80	4.5E-6	60	-	20.0
10049	1.0	1.5	80	1.0E-6	3960	-	19.9
10050	1.0	1.5	80	3.0E-6	150	-	20.0
10051	1.0	1.5	80	3.0E-4	5	20	20.1
10052	1.0	1.5	80	2.0E-4	5	50	20.0
10053	1.0	1.5	80	3.0E-4	5	120	20.0
10055	1.0	1.5	80	5.0E-4	5	-	19.9
10056	1.0	1.5	80	3.6E-6	120	-	19.9
10057	1.0	1.5	80	7.7E-7	7200	-	19.9
10058	1.0	1.5	80	7.7E-7	2880	20	19.9

Shot	Gap [mm]	Cathode radius [mm]	Vcharge [kV]	Vac [Torr]	Time under vacuum [min]	Time between vacuum storage and install [min]	Load conductivity [mS/cm]
10059	1.0	1.5	80	9.0E-6	120	-	19.6
10060	1.0	1.5	80	5.0E-4	5	-	19.6
10061	1.0	1.5	80	2.7E-6	1200	-	19.6
10062	1.0	1.5	80	7.0E-4	5	-	19.9
10063	1.0	1.5	80	6.0E-5	5	-	19.5
10064	0.6	1.5	80	1.2E-5	133	-	19.6
10065	1.0	1.5	80	1.6E-6	945	-	19.6
10066	1.0	1.5	80	5.0E-5	10	35	19.6
10067	0.6	1.5	80	5.7E-6	123	-	19.6
10068	1.2	1.5	80	7.0E-6	140	-	19.6
10069	1.0	1.5	80	5.0E-4	5	30	19.6
10070	0.8	1.5	80	9.5E-6	115	-	20.0
10071	0.8	1.5	80	8.5E-6	100	-	20.5
10072	1.0	1.5	80	5.4E-4	5	-	20.6
10073	0.6	1.5	80	4.1E-6	720	-	20.6
10075	1.0	1.5	80	6.0E-4	5	-	20.6
10076	1.0	1.5	80	1.0E-4	5	25	20.6

REFERENCES

1. W. A. Stygar et al., *55-TW magnetically insulated transmission-line system: Design, simulations, and performance*, Phys. Rev. ST Accel. Beams 12, 120401, 2009.
2. M. E. Savage et al., *An overview of pulse compression and power flow in the upgraded Z pulsed power driver*, in Proceedings of the 16th IEEE International Pulsed Power Conference, (IEEE, Albuquerque, NM, 2007), p. 979.
3. M. E. Savage et al., *Status of the Z pulsed power driver*, in IEEE Pulsed Power Conference 2011, Chicago, IL, 2011, p. 983.
4. T. W. L. Sanford, *Measurement of electron energy deposition necessary to form an anode plasma in Ta, TI, and C for coaxial bremsstrahlung diodes,* J. Appl. Phys., vol. 66, p. 10, 1989
5. M. E. Cuneo, *The effect of electrode contamination, cleaning and conditioning on high-energy pulsed-power device performance*, IEEE Transactions on Dielectrics and Electrical Insulation, vol. 6, no. 4, p. 469, 1999.
6. K. LeChien et al., *A 1-MV, 1-MA, 0.1-Hz linear transformer driver utilizing an internal water transmission line*, in IEEE Pulsed Power Conference 2009, Washington, DC, 2009, p. 1186.
7. M. G. Mazarakis et al., *Experimental validation of the first 1-MA water-insulated MYKONOS LTD voltage adder*, in Pulsed Power Conference 2011, Chicago, IL, 2011, p. 625.
8. M. E. Savage et al., *Temporally shaped current pulses on a two-cavity linear transformer driver system*, in Pulsed Power Conference 2011, Chicago, IL, 2011, p. 844.
9. B. T. Hutsel, et al., *Transmission-line-circuit model of an 85-TW, 25-MA pulsed-power accelerator*, Phys. Rev. Accel. Beams 21, 030401, March 23 2018.
10. B. T. Hutsel et al., *Millimeter-gap magnetically insulated transmission line power flow experiments,* in 2015 IEEE Pulsed Power Conference (PPC), Austin, TX, 2015, p. 1.
11. D. D. Hinshelwood, *BERTHA: A Versatile Transmission Line and Circuit Code*, Naval Research Laboratory memorandum Report No. 5185, 1983.
12. Chicago is being developed by Voss Scientific with partial support from the Defense Advanced Research Projects Agency under Contract No. W31P4Q-15-C-0055 and the Air Force Office of Scientific Research under Contract No. FA9550-14-C-0034.
13. A. Kim, et al., *Prefire probability of the switch type Fast LTD*," in IEEE Pulsed Power Conference 2009, Washington, DC, 2009, p. 565.
14. A. A. Kim, et al., *Development and tests of fast 1-MA linear transformer driver stages*, Phys. Rev. ST Accel. Beams 12, 050402, 2009.
15. W. A. Stygar, et al., *Energy loss to conductors operated at lineal current densities ≤10 MA/cm: Semianalytic model, magnetohydrodynamic simulations, and experiment*, Phys. Rev. ST Accel. Beams 11, 120401, 2008

16. M. S. Di Capua and D. G. Pellinen, *Propagation of power pulses in magnetically insulated vacuum transmission lines,* J. Appl. Phys. 50, 3713, 1979.

17. T. C. Wagoner, et al., *Differential-output B-dot and D-dot monitors for current and voltage measurements on a 20-MA, 3-MV pulsed-power accelerator*, Phys. Rev. ST Accel. Beams 11, 100401, 2008.

18. D. V. Rose, et al. Manuscript in preparation (2018).

19. C. Thoma, C. L. Miller, D. Offermann, R. E. Clark, E. A. Madrid, D. R. Welch, and W. A. Stygar, Simulations of neutron production from charged-particle diodes, Voss Scientific Internal Memo May 2015.

DISTRIBUTION

1	MS0899	Technical Library	9536 (electronic copy)
1	MS0359	D. Chavez, LDRD Office	1911 (electronic copy)

Sandia National Laboratories